Magnon component of the resistivity in single-crystal terbium-yttrium alloys

K. P. Belov, S. A. Nikitin, V. P. Posyado, and G. E. Chuprikov

Moscow State University

The resistivity of crystals of terbium-yttrium alloys was investigated in a wide range of concentrations at temperatures from 4.2 to 400°K. The magnon part of the resistivity was separated. The effective mass of the conduction electrons m^* and the s-f exchange parameter were calculated on the basis of the formulas of the indirect-exchange theory. A change was observed in the Fermi surface in the concentration region (40–50) at.%Y, thus indicating a strong connection between the structure of the Fermi surface and the magnetic properties of the terbium-yttrium alloys. It is shown that the residual resistivity due to the spin disorder ρ_M^{res}, greatly exceeds the electrostatic contribution to ρ_{res}.

The investigation of the electric properties of single crystals of rare-earth (RE) alloys is of considerable interest for the theory of magnetism. The resistivity of RE alloys has been investigated so far using polycrystalline samples, [1–5] and only several studies were made with single crystals. [6–8] Measurements with polycrystalline samples do not yield complete and reliable information on the conduction-electron scattering mechanisms in these substances, because the resistivity of RE alloys and metals exhibits in principle different behaviors in different crystallographic directions, making it difficult to compare the conclusions of the indirect exchange theory with the experimental data.

An important circumstance is that the experimental investigation of the Fermi surfaces of RE metals and alloys with the aid of the galvanomagnetic effect and resonant methods is presently made difficult by the insufficient purity of the samples. The study of the electric properties yields useful information on the deformation of the Fermi surface when RE metals are alloyed. As shown by Dzyaloshinskiĭ, [9] the magnetic properties of RE metals are strongly connected with the singularities of the Fermi surface and with the electronic structure in these metals. Thus, simultaneous study of the electric and magnetic properties can yield a more complete idea on the nature of the ferromagnetism and of helicoidal antiferromagnetism in these substances.

We have investigated the resistivity of single crystals of terbium–yttrium alloys in a wide range of concentrations at temperatures from 4.2 to 400 °K.

The single crystals were grown by drawing from the melt (by the Czochralski method). The samples for the measurements were cut from the single crystals with a diamond disk in three crystallographic directions, $\langle 10\bar{1}0 \rangle$, $\langle 11\bar{2}0 \rangle$, $\langle 0001 \rangle$, after which the samples were etched in a solution of nitric acid in alcohol. In addition, to relieve the internal stresses, all samples were annealed at 600 °C for 24 hours in a vacuum not worse than 10^{-5} mm Hg.

An analysis of the impurity concentrations has shown that the oxygen, hydrogen, and nitrogen contents do not exceed 0.005, 0.0005, and 0.006 wt.%, respectively,

and the total concentration of the metallic impurities was not larger than 0.01 wt.%. By determining the terbium concentration in longitudinal and transverse sections, it was established that the components are uniformly distributed in length and in the cross section of the single crystals. The orientation along the indicated crystallographic directions was by the Laue method with an error of 1°, and in some cases with greater accuracy by using a diffractometer.

The resistivity was measured by a standard four-contact method using a potentiometer circuit. The samples were rectangular with area 10^{-2} cm^2 and length 0.8–1.0 cm.

For all the investigated alloys an abrupt change in the value of $d\rho/dT$ was observed in the basal plane (crystallographic directions $\langle 10\bar{1}0 \rangle$ and $\langle 11\bar{2}0 \rangle$ or respectively b and a) at the point Θ_2 of phase transition from the paramagnetic state into the antiferromagnetic state, and at the point Θ_1 of the phase transition from the antiferromagnetic state into the ferromagnetic state (Fig. 1). At the point Θ_2 the value of $d\rho/dT$ increased upon cooling below Θ_2, and at the point Θ_1 the value of $d\rho/dT$ decreased upon cooling below Θ_1, the change of $d\rho/dT$ at the point Θ_2 being much larger than at the point Θ_1. Along the crystallographic direction $\langle 0001 \rangle$ (the c axis), for all the alloys, a maximum of the resistivity with a change of the character of the conductivity is observed near Θ_2, namely $d\rho/dT < 0$ in a certain temperature interval below Θ_2.

In accordance with the Matthiesen rule, the total resistivity of ferromagnetic metals $\rho(T)$ is given by[3,10]

$$\rho(T) = \rho_{res} + \rho_{ph}(T) + \rho_e(T) + \rho_M(T), \tag{1}$$

where ρ_{res} is the residual resistivity, $\rho_e(T)$ is the resistivity due to electron–electron scattering, and $\rho_{ph}(T)$ and $\rho_M(T)$ are the resistivities due to the scattering of the electrons by the phonons and magnons, respectively.

To separate the resistivity due to the scattering of the conduction electrons by the spin inhomogeneities, it is necessary to determine the temperature-dependent contributions $\rho_{ph}(T)$ and $\rho_e(T)$. This can be done by us-
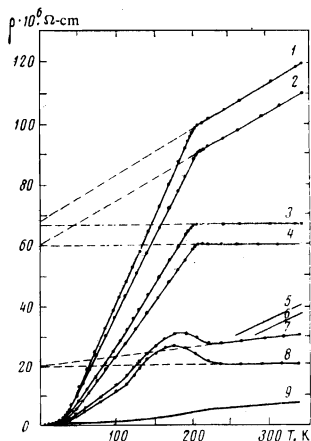
FIG. 1. Resistivity of single crystal of the alloy Tb—16.5 at.% Y. Curves 1, 2, 7 represent $\rho(T) - \rho_{res}$ along the respective crystallographic directions $\langle 10\bar{1}0 \rangle$, $\langle 11\bar{2}0 \rangle$, $\langle 0001 \rangle$; curves 3, 4, and 8 represent the magnon contribution $\rho_M(T)$ to the resistivity along these directions; curves 5, 6, and 9 represent the contribution $\rho_{ph}(T)$ due to scattering by phonons along the same directions.

ing data on the temperature dependence of the resistivity of metals that have a similar electronic structure and have no magnetic ordered state.[10] For heavy RE metals, such a metal is lutecium, which has a Fermi surface similar to those of Tb, Dy, and Er.[11] As shown by Vol'kenshteĭn and co-workers, [10] by using $\rho_e(T)$ and $\rho_{ph}(T)$ of lutecium it is possible to separate $\rho_M(T)$ of heavy RE metals.

For alloys with large yttrium content it is natural to assume that their Fermi surfaces are similar to the Fermi surface of yttrium. The contributions $\rho_e(T)$ and $\rho_{ph}(T)$ were separated for Lu and Y with the aid of a known expression[10] that is valid for $T < 0.1\Theta_D$:

$$\rho(T) = \rho_{res} + AT^2 + BT^5, \qquad (2)$$

where A is a parameter characterizing the electron-electron scattering and B determines the scattering by phonons. We used the results of the measurements of the resistivity of single-crystal yttrium and the published data for $\rho(T)$ of polycrystalline and single-crystal lutecium. [12,13] By plotting in the temperature interval 4.2–25 °K the dependence of $(\rho(T) - \rho_{res})/T^2$ on T^3 for Lu and Y, respectively, we determined the experimental values of A and B along the c axis and in the basal plane.

The contribution from the electron-phonon scattering $\rho_{ph}(T)$ can be calculated in a wide range of temperatures from the Bloch–Gruneisen function, [14] which is determined by the quantity B and by the characteristic temperature Θ. The values of Θ were determined from the relation

$$\frac{\rho_{ph}(T_i)}{\rho_{ph}(T_2)} = \frac{497.6}{\Theta^6} \frac{T_i^5}{T_2} \qquad (3)$$

Here $\rho_{ph}(T_1)$ is the contribution to the resistivity from the scattering by phonons at a temperature $T_1 < 0.1\Theta_D$; $\rho_{ph}(T_2)$ is the contribution to the resistivity from scat-

tering by phonons at the temperature $T_2 > 0.5\Theta_D$. The characteristic temperatures in the basal plane and for the c direction in Lu, obtained from formula (3), are $\Theta^\perp = 147$ K and $\Theta^{||} = 170$ K, while for Y they are $\Theta^\perp = 176$ K and $\Theta^{||} = 199$ K, respectively. The obtained value of $\Theta^\perp$ for single-crystal Lu is close to the value of the characteristic temperature obtained earlier[15] for polycrystalline Lu, while the values of $\Theta^{||}$ for Lu and Y are close to the Debye temperatures calculated from the heat capacity (for Lu and Y we have $\Theta_D = 166$ K and $\Theta_D = 218$ K, respectively).

Starting from the obtained values of B and Θ, we used the Bloch–Gruneisen formulas[14] to calculate $\rho_{ph}(T)$, and then relation (1) to calculate $\rho_e(T)$ for Lu and Y along the crystallographic axes. According to our results, the electron-electron scattering in yttrium and lutecium have similar temperature dependences, while the values of ρ_e and $d\rho_e/dT$ at room temperature are quite close.

As follows from the theory, [16,17] in the paramagnetic region far from Θ_2, the resistivity ρ_M does not depend on the temperature $d\rho_M/dT$. We can trace the variation of the Fermi surface of the Tb–Y in the course of alloying by using the known relation[10]

$$\frac{d\rho_{ph}^i}{dT} \sim \left(\sum_s dS_i \right)^{-1}, \qquad (4)$$

where i is the crystallographic direction (axes a, b, c), and $\sum_s dS_i$ are the projections of the Fermi surface on planes normal to the axes a, b, and c.

It is seen from Fig. 2 that the quantity $d\rho/dT = d\rho_{ph}/dT + d\rho_e/dT$ remains practically the same for alloys with yttrium content up to 40 at.%, while for alloys with more yttrium (more than 50 at.%) the value of $d\rho/dT$ increases and approaches with decreasing terbium to the value of $d\rho/dT$ of yttrium. This behavior of $d\rho/dT$ seems to indicate that the Fermi surfaces of terbium and of alloys containing less than 40 at.% Y are practically the same. In addition, it can be noted that the ratio $(d\rho^\perp/dT)(d\rho^{||}/dT)^{-1}$, which characterizes the ratio of the areas $\Sigma dS^{||}/\Sigma dS^\perp$ of the projection of the Fermi surface on planes perpendicular and parallel to the c axis, changes noticeably near an yttrium concentration close to 50 at.%.

Starting from the foregoing estimate of the change in the electronic structure of the Tb:Y alloys, we have
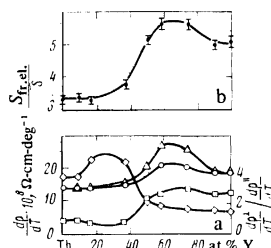

FIG. 2. a) Concentration dependence of $d\rho/dT$ in the paramagnetic region along the crystallographic directions ($\triangle - \langle 10\bar{1}0 \rangle$, $\circ - \langle 11\bar{2}0 \rangle$, $\square - \langle 0001 \rangle$) and of the ratio $(d\rho^\perp/dT) \cdot (d\rho^{||}/dT)^{-1}$ — curve $\diamond$); b) concentration dependence of the quantity $S_{tr.el}/S$.

TABLE I. Contribution made to the resistivity by the spin disorder in the paramagnetic state.*

Composition, at.%	$(\rho_M)_{max} \cdot 10^6$, Ω-cm					
	Linear extrapolation			Separation		
	b	a	c	b	a	c
Tb	—	90	67	—	71	67
Tb—9 at.% Y	89	70	44	82	68	42.5
Tb—16.5 at.% Y	68	60	20	66.5	58	19.5
Tb—37.0 at.% Y	61	57	38	60	54	38
Tb—50.0 at.% Y	47	—	28	49.5	—	32
Tb—58.0 at.% Y	39	31	5	39	29.5	7.5
Tb—74.0 at.% Y	27	16	1	26	16	4.0
Tb—90.0 at.% Y	7	3	-4	9	5	1.5

*The data for Tb are from[10].

FIG. 4. Magnon resistivity components in the paramagnetic region for TB-Y alloys: △—⟨10$\bar{1}$0⟩, o—⟨11$\bar{2}$0⟩, □—⟨0001⟩.

assumed, in order to separate $\rho_M(T)$, that alloys with up to 40 at.% Y make the same contribution to the resistivity as $\rho_e^i(T)$ for lutecium, and when the yttrium content is 50 at.% and larger, the contribution $\rho_e^i(T)$ is the same as for yttrium. To resolve the phonon part of the resistivity along the crystallographic directions it is necessary to determine the characteristic temperatures for the given alloy. According to the Bloch model, the scattering of the conduction electrons by the crystal-lattice vibrations in the temperature region $T > 0.5\Theta_D$ can be represented in the form

$$\rho_{ph}^{all}(T) = KT/4M_{all}\Theta_{all}^2 , \qquad (5)$$

where K is a constant proportional to the Debye radius and M is the mass of the ion.

Since the radius of the Debye sphere is inversely proportional to the crystal-lattice parameters, it follows that Lu, Tb, and Y can be assumed to have the same value of K, with an error not larger than 3%. For
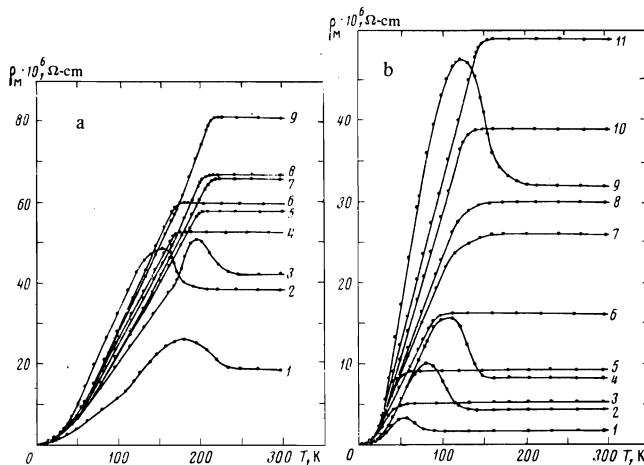
alloys containing yttrium up to 40 at.% we then have

$$\rho_{all.ph}^i(\Theta_{all}^i) = \frac{M_{Lu}\Theta_{Lu}^i}{M_{all}\Theta_{all}^i}\rho_{Lu}^i(\Theta_{Lu}^i), \qquad (6)$$

$$\Theta_{all}^i = \left(\frac{M_{Lu}\Theta_{Lu}^i\rho_{Luph}^i(\Theta_{Lu}^i)}{M_{all}d\rho_{all.ph}^i/dT}\right)^{1/3}, \qquad (7)$$

$$\frac{d\rho_{all.ph}^i}{dT} = \frac{d\rho^i}{dT} - \frac{d\rho_{eLu}^i}{dT} \qquad (8)$$

Here (8) is valid for the paramagnetic region of temperatures far from Θ_2. We can write similar formulas for alloys with more than 50 at.% yttrium. Using (6)–(8) and the tabulated function $\rho_{ph}(T)/\rho_{ph}(\Theta) = f(T/\Theta),$ [14] we have calculated the characteristic temperatures and the resistivities $\rho_{ph}(T)$ due to the electron–phonon scattering for the three crystallographic directions in each of the alloys.

Table I lists the values of $(\rho_M)_{max}$, which is a part of the resistivity due to the total magnetic disorder in the paramagnetic region; these values were obtained by linear extrapolation to $T = 0$ (see Fig. 1) and by subtraction of $\rho_e^i(T) + \rho_{ph}^i(T)$ from the total resistivity:

$$\rho_M^i(T) = \rho^i(T) - \rho_{res}^i - \rho_{ph}^i(T) - \rho_e^i(T). \qquad (9)$$

For alloys with yttrium content up to 40 at.% it is possible to separate $\rho_e + \rho_{ph}$ for the c direction only under the additional assumption that

$$\left(\frac{d\rho_e}{dT}\right)_{Lu}\left(\frac{d\rho_{ph}}{dT}\right)_{Lu}^{-1} = \left(\frac{d\rho_e}{dT}\right)_{all}\left(\frac{d\rho_{ph}}{dT}\right)_{all}^{-1} ,$$

and the values of $(\rho_M)_{max}$ obtained in this manner differ little from the values of $(\rho_M)_{max}$ determined by linear extrapolation.

It is seen from the table that linear extrapolation cannot be used for alloys with large yttrium contents. Figure 1 shows the temperature dependence of the contributions $\rho_e + \rho_{ph}$ and ρ_M to the resistivity, obtained by the method described above.

The temperature coefficient for $\rho_M(T)$ changes at the phase-transition points Θ_1 and Θ_2, this change being much smaller at the point Θ_1 than at the point Θ_2. When the yttrium content is increased to 16 at.%, an increase in the anisotropy of $\rho_M(T)$ is observed (Fig. 3a and Fig. 4). For alloys Tb—16.5 at.% Y, $(\rho_M^{\perp})_{max}$ is almost three times larger than $(\rho_M^{\parallel})_{max}$. With further increase of the yttrium content, the difference between $\rho_M^{\perp}$ and $\rho_M^{\parallel}$ decreases, and for the alloy Tb—50 at.% Y it is minimal (Fig. 3b and Fig. 4). Alloys with large yttrium content

FIG. 3. Magnon resistivity component $\rho_M(T)$ for Tb-Y single crystals: a) Tb—9 at.% Y: 3—⟨0001⟩, 7—⟨11$\bar{2}$0⟩, 9—⟨10$\bar{1}$0⟩, Tb—16.5 at.% Y: 1—⟨0001⟩, 5—⟨11$\bar{2}$0⟩, 8—⟨10$\bar{1}$0⟩; Tb—37 at.% Y: 2—⟨0001⟩, 4—⟨11$\bar{2}$0⟩, 6—⟨1$\bar{0}$10⟩; b) Tb—50 at.% Y: 9—⟨0001⟩, 11—⟨1$\bar{0}$10⟩, Tb—58 at.% Y: 4—⟨0001⟩, 8—⟨11$\bar{2}$0⟩, 10—⟨10$\bar{1}$0⟩; Tb—74 at.% Y: 2—⟨0001⟩, 6—⟨11$\bar{2}$0⟩, 7—⟨10$\bar{1}$0⟩; Tb—90 at.% Y: 1—⟨0001⟩, 3—⟨11$\bar{2}$0⟩, 5—⟨10$\bar{1}$0⟩.
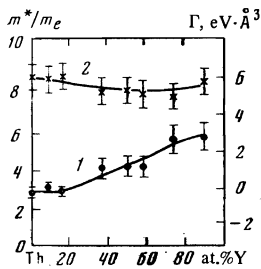
FIG. 5. Concentration dependence of the $s-f$ exchange parameter (curve 1) and of the effective mass of the conduction electrons in the basal plane (curve 2).

have an anisotropy of ρ_M in the basal plane, which in these alloys is comparable with the anisotropy of ρ_M between the c direction and the direction perpendicular to it.

The magnetic part of the resistivity in the paramagnetic region $(T > \Theta_2)$ for the directions a and b, $(\rho_M^a)_{max}$ and $(\rho_M^b)_{max}$ respectively, decreases linearly with increasing yttrium content, but along the c direction the dependence of $(\rho_M^c)_{max}$ on the yttrium concentration is more complicated (Fig. 4). In the concentration region ~50 at.% Y, where a restructuring of the Fermi surface takes place, an increase of $(\rho_M^c)_{max}$ is observed, but with further increase of the yttrium content (more than 60 at.%) the value of $(\rho_M^c)_{max}$ decreases monotonically.

In the indirect-exchange theory, the magnetic and the electric properties are closely related: ρ_M and Θ_p depend on the same microscopic parameters. For the magnetic part of the resistivity $(\rho_M)_{max}$ due to the spin disorder in the paramagnetic state at $T > \Theta_2$, an analytic expression was obtained in[16,17]. For alloys with yttrium this expression takes the form

$$(\rho_M)_{max} = \frac{3\pi}{4\hbar^3 e^2} \frac{\Gamma^2 m^{*2}}{v_0 k_f^2}(g_I - 1)^2 I x (1 + I x),\qquad (10)$$

where Γ is the parameter of the $s-f$ exchange, m^* is the effective mass of the conduction electron, v_0 is the atomic volume, k_f is the Fermi wave vector, I is the total magnetic moment of the ion, and x is the concentration of the magnetic ions.

Within the framework of the indirect-exchange theory, an expression was obtained for the paramagnetic Curie temperature[18]

$$\Theta_p = \frac{3\pi n_a^2}{2k_B\hbar^3} \frac{\Gamma^2 m^*}{v_0^2 k_f^2}x(g_I - 1)^2$$

$$\times I(I+1)\sum_{n\neq m} F(2k_f R_{nm}),\qquad (11)$$

where n_a is the number of conduction electrons per atom and

$$\sum_{n\neq m} F(2k_f R_{nm})$$

is the lattice sum, the value of which for rare-earth metals is $(6.94 \pm 0.03) \cdot 10^{-3}$.

With the aid of formulas (10) and (11) and the experimental data for $(\rho_M)_{max}$, as well as the paramagnetic Curie temperatures Θ_p previously determined for Tb–Y

alloys, [19-21] we have calculated the effective mass of the conduction electrons m^* and the $s-f$ exchange parameter for Tb–Y alloys.

Figure 5 shows the concentration dependence of the reduced effective mass of the electron m^*/m_e (m_e is the mass of the free electron). For pure terbium and for the alloys Tb—9 at.% Y and Tb—16.5 at.% Y, the value of m^*/m_e is ~3, in agreement with the previously determined values of m^*/m_e for heavy RE metals[17] and for Gd–Y alloys.[5] For alloys with more than 40 at.% yttrium, the ratio m^*/m_e increases noticeably with increasing yttrium concentration, reaching the value 5.8 for the alloy Tb—90 at.% Y. The $s-f$ exchange parameter for terbium–yttrium alloys is practically independent of the concentration within the limits of errors (Fig. 5).

Definite information on the deformation of the Fermi surface when terbium is alloyed with yttrium can be obtained by estimating the deviation of the area of the real Fermi surface S from the area of the Fermi surface of the free electrons $S_{fr.el}$, using the relation[22]

$$S_{fr.el}/S = Z^{1/2}/n_a^{1/2}.\qquad (12)$$

Here $S_{fr.el}$ is the area of a certain hypothetical spherical Fermi surface in the presence of n_a free electrons per atom, and Z is the Ziman parameter:

$$Z = \frac{4e^2 M k_B \Theta_D^2}{\pi^3 \hbar^3 2^{-1/3} D} \frac{d\rho_{ph}}{dT},\qquad (13)$$

where M is the atomic weight (the mass of the ion), k_B is the Boltzmann constant, Θ_D is the Debye temperature, and D is the Debye radius.

The Ziman parameter was calculated for each alloy with the aid of the values obtained by us for $d\rho_{ph}/dT$ in the paramagnetic region. The values of Θ_D and D were taken for the alloys by using linear interpolation from the value for pure metals ($\Theta_D = 182$ K, $D^{-1} = 1.23 \cdot 10^8$ cm^{-1} for terbium and $\Theta_D = 218$ K, $D^{-1} = 1.21 \cdot 10^8$ cm^{-1} for yttrium).

Figure 2 shows the variation of the ratio $S_{fr.el}/S$ with changing yttrium concentration. For alloys with (40–50) at.% Y, an abrupt change of the Ziman parameter and of the ratio $S_{fr.el}/S$ is observed.

Figure 6 shows the concentration dependence of the residual resistivity ρ_{res}. The values of ρ_{res} for terbium alloys with (50–70) at.% yttrium are quite high and close to the values of ρ_{res} for Gd–Y alloys in the gadolinium concentration region (40–60) at.%.[3] The dependence of ρ_{res} on the concentration for single-crystal Tb–Y alloys cannot be described by a relation of the $x(1-x)$ type. A concentration dependence closest to this type is observed by ρ_{res} only in the c direction, but $\rho_{res}^a(x)$ and $\rho_{res}^b(x)$ have different forms. The experimental values of ρ_{res} for the crystallographic directions a, b, and c in the Tb–Y system can be described with the aid of a relation of the $a + bx + cx^2 + dx^3$:

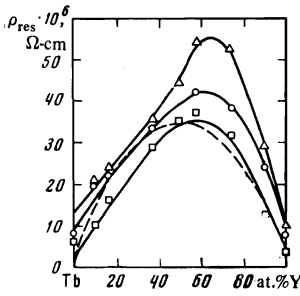FIG. 6. Residual resistivity of single crystal Tb–Y alloys along the following crystallographic directions: △—$\langle 10\bar{1}0 \rangle$, ○—$\langle 11\bar{2}0 \rangle$, □—$\langle 0001 \rangle$. Solid lines—relations of the type $a + bx + cx^2 + dx^3$. Dashed line—relation of the type $x(1-x)$ for the $\langle 0001 \rangle$ direction.

$$\rho_{res}^{b} = 9 + 258x - 441x^2 + 183x^3;$$

$$\rho_{res}^{a} = 10 + 182x - 306x^2 + 124x^3; \tag{14}$$

$$\rho_{res}^{c} = 3 + 177x - 288x^2 + 111x^3.$$

The residual resistivity of rare-earth metals and their alloys, with both magnetic and nonmagnetic metals, was investigated theoretically by Dekker.[17] According to his results, the residual resistivity can be represented in the form of a sum of two terms:

$$\rho_{res} = \rho_{st}^{res} + \rho_{M}^{res}, \tag{15}$$

$$\rho_{st}^{res} = \frac{3\pi m^* V_{ab}^2}{8e^2\hbar E_i v_0} x(1-x), \tag{16}$$

$$\rho_{M}^{res} = \frac{3\pi m^* \Gamma^2 (g_i-1)^2 I^2}{8e^2\hbar E_i v_0} x(1-x), \tag{17}$$

where ρ_{st}^{res} is the electrostatic contribution to ρ_{res}, ρ_{M}^{res} is the residual resistivity due to the spin disorder, x is the fraction of the magnetic ions in the alloy, and $V_{ab} = V_a - V_b$, where V_a and V_b are the Coulomb potentials of the terbium and yttrium ions.

Combining formulas (10) and (17), we easily obtain the concentration dependence of ρ_{M}^{res}:

$$\rho_{M}^{res}(x) = \frac{I(1-x)}{1+xI} (\rho_M)_{max}. \tag{18}$$

Substituting the obtained values of $(\rho_M)_{max}$, we used formula (18) to calculate the values of ρ_{M}^{res} for all the investigated compositions (Fig. 7). The values of ρ_{st}^{res} were obtained in accordance with formula (15) by subtracting ρ_{M}^{res} from ρ_{res} (curve 1 minus curve 2, Fig. 7). The character of the $\rho_{st}^{res}(x)$ dependence is quite close to that predicted by the Nordheim and Dekker rule.[17] The electrostatic contribution to the residual resistivity increases when yttrium is added to the terbium, but decreases at a large yttrium content. V_{ab} can be calculated from formulas (16) and (17):

$$V_{ab} = \Gamma(g_i - 1) I (\rho_{st}^{res}/\rho_{M}^{res})^{1/2}. \tag{19}$$

An estimate of V_{ab} by formula (19) yields ~ 5.23 eV-$\mathring{A}^3$. It is seen from Fig. 7 that the quantity ρ_{res} for the Tb–Y alloys is determined mainly by the contribution ρ_{M}^{res} due to the magnetic disorder. The empirically obtained con-
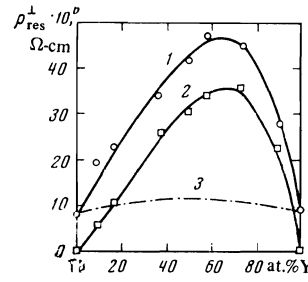

FIG. 7. Residual resistivity in the basal plane ρ_{res} (curve 1), the magnetic component of the residual resistivity in the basal plane ρ_{M}^{res} (curve 2), and $(\rho_{res} - \rho_{M}^{res})$ (curve 3).

centration dependences of ρ_{res} (formulas (14)) can be obtained from (17) by taking into account the concentration dependences of m^* and Γ.

In addition, ρ_{res} receives a contribution ρ_{st}^{res} from structural imperfections. This contribution can be estimated for pure components, for which $\rho_{M}^{res} = \rho_{st}^{res} = 0$. All the single crystals were prepared from the same original metals and grown under the same conditions, so that ρ_{st}^{res} can be assumed to be practically constant in the entire concentration region.

The results of the present investigation of the electric properties of rare-earth terbium–yttrium alloys show that, despite the fact that the terbium and yttrium ions have similar electron shells and close values of the crystal-lattice parameters, a substantial deformation of the Fermi surface takes place when these metals are alloyed, in the concentration region (40–50) at.% Y, and leads to a change in the effective mass of the electrons m^*, and to a nonmonotonic concentration dependence of ρ_M^c. The $s-f$ exchange parameter for the basal plane remains in this case practically constant and is not very sensitive to the shape of the Fermi surface.

As shown by investigations of magnetic and magnetostriction properties,[23] at an yttrium concentration larger than ~ 30 at.% the ferromagnetism vanishes and the alloys remain antiferromagnetic with helicoidal structure down to the lowest temperatures. These data and the results of the present investigation point to a strong relation between the singularities of the Fermi surface and the magnetism of the RE metals or their alloys, in agreement with Dzyaloshinskiĭ's theory.[9]

Thus, the contribution made to the resistivity by the mechanism of conduction-electron scattering by the spin disorder is quite large in Tb–Y alloys, both in the paramagnetic region and at low temperatures, even near $0\,°K$, as indicated by the large values of $(\rho_M)_{max}$ and ρ_M^{res}. With increasing content of the nonmagnetic yttrium, however, the role of this mechanism decreases gradually.

[1]F. A. Smidt and A. H. Daane, Jr., J. Phys. Chem. Solids 24, 316 (1963).
[2]J. Hennephof, Phys. Lett. 11, 273 (1964).
[3]I. Popplewell, P. G. Arnold, and P. M. Davies, Proc. Phys. Soc. Lond. 92, 177 (1967).

[4]T. Sugawara, J. Phys. Soc. Jap. **20**, 2252 (1967).
[5]P. G. Arnold and J. Popplewell, J. Phys. F **3**, 1985 (1973).
[6]S. A. Nikitin, S. S. Slobodchikov, and O. D. Chistyakov, Zh. Eksp. Teor. Fiz. **70**, 104 (1976) [Sov. Phys. JETP **43**, 54 (1976)].
[7]I. Tokcshi, Sci. Inst. Hiroshima Univ. Ser. A 376107 (1973).
[8]A. Mishima, H. Tujii, and T. Okamoto, J. Phys. Soc. Jpn. **38**, 837 (1975).
[9]I. E. Dzyaloshinskiĭ, Zh. Eksp. Teor. Fiz. **47**, 336 (1964) [Sov. Phys. JETP **20**, 223 (1965)].
[10]N. V. Volkenstein, V. P. Dyakina, and V. E. Startsev, Phys Status Solidi **57**, 9 (1973).
[11]S. C. Keeton and T. L. Loucks, Phys. Rev. **168**, 672 (1968).
[12]D. W. Boys and S. Legvold, Phys. Rev. **174**, 174 (1968).
[13]A. R. Mackintoch, Phys. Lett. **4**, 140 (1963).
[14]G. K. White, Experimental Techniques in Low Temperature Physics, Oxford, 1958 (Russ. transl. Fizmatgiz, 1961, p. 331).

[15]N. V. Volkenshteĭn and V. P. Dyakina, Zh. Eksp. Teor. Fiz. **59**, 1160 (1970) [Sov. Phys. JETP **32**, 633 (1971)].
[16]P. G. De Gennes, J. Phys. (Paris) **23**, 510 (1962).
[17]A. J. Dekker, J. Appl. Phys. **36**, 906 (1965).
[18]T. Kasuja, Magnetism 11B, New York, Academic Press,, 1966, p. 215.
[19]S. Weinstein, R. S. Craig, and W. E. Wallace, J. Chem. Phys. **39**, 1449 (1963).
[20]H. Nagasawa and T. Sugawara, J. Phys. Soc. Jpn. **23**, 711 (1967).
[21]M. Darby and K. N. Taylor, Physics of Rare Earth Solids, Halsted, 1972 (Russ. transl. Mir, 1974, p. 170).
[22]J. M. Ziman, Electrons and Phonons, Oxford, 1960.
[23]K. P. Belov, R. Z. Levitin, S. A. Nikitin, and L. I. Solntseva, Zh. Eksp. Teor. Fiz. **54**, 384 (1968) [Sov. Phys. JETP **27**, 207 (1968)].

Observation of the suppression of a nuclear reaction in a direct beam of γ quanta

G. V. Smirnov, N. A. Semioshkina, V. V. Sklyarevskiĭ, S. Kadechkova, and B. Shestak

I. V. Kurchatov Institute of Atomic Energy
(Submitted May 19, 1976)
Zh. Eksp. Teor. Fiz. **71**, 2214–2229 (December 1976)

The suppression of a nuclear reaction upon resonant interaction of γ quanta with a regular system of nuclei was observed in a direct beam of γ quanta passing through a perfect crystal. γ quanta of the Mössbauer transition in Fe^{57} nuclei and iron crystals enriched up to 85% by resonant Fe^{57} nuclei were utilized in the experiment. A consequence of the suppression of the reaction was a sharp increase in the transmittance of the crystal for resonant γ quanta in an angular range of 30″ in the neighborhood of the Bragg angle.

PACS numbers: 76.80.+y

INTRODUCTION

Previously unknown collective nuclear phenomena were predicted[1-3] on the basis of conservation of coherence during resonant nuclear scattering of Mössbauer γ quanta. Among the more striking effects in which an aggregate of nuclei behave as a single ensemble, one can single out the suppression of nuclear reactions (SNR) or the Kagan–Afanas'ev effect. In the example of this and other effects, Kagan and Afanas'ev showed that the nuclear parameters of the ensemble, such as the position of the resonant level, the lifetime of the excited state, the relationship between the partial widths of the nuclear levels, and so forth, may differ significantly from the corresponding parameters of the individual nucleus entering into the composition of the ensemble.

SNR should appear upon the interaction of resonant γ quanta with the nuclei in perfect crystals. Under these conditions the γ quanta are captured in a regular system of identical nuclei. The excitation which appears in such a system upon capture of an individual γ quantum cannot be associated with one or the other specific nucleus. In accordance with the quantum mechanical principle of superposition of states, it must pertain with a definite probability to each nucleus in the system and thus envelops the entire system as a whole. A collective excited state of the nuclear system appears.[2]

In virtue of the conservation of coherence during the lifetime of the collective state, the emission of a γ quantum upon decay of the collective state only takes place in certain directions. These directions are specified by the symmetry of the regular system of nuclei. In this connection it is essential that the probability for the emission of a quantum increases significantly in comparison with the probability for elastic decay of an isolated nucleus, whereas the probability for transfer of the excitation energy to a conversion electron (inelastic reaction channel) remains the same as before.

Upon fulfillment of the Bragg conditions for an incident γ quantum, elastic decay in an excited nuclear system can take place in two directions, as a consequence of which an abrupt rearrangement of the γ quantum state takes place on entrance into the crystal. A pair state appears which corresponds to the wave field representing a coherent superposition of two plane waves. Below, in connection with the propagation of this field in a crys-